

# Pharmacological Evaluation of Iodo and Nitro Analogs of $\Delta^8$ -THC and $\Delta^9$ -THC

BILLY R. MARTIN,\*<sup>1</sup> DAVID R. COMPTON,\* SIMON F. SEMUS,†  
SONYUAN LIN,‡ GILBERT MARCINIAK,‡ JOLANTA GRZYBOWSKA,‡  
AVGUI CHARALAMBOUS‡ AND ALEXANDROS MAKRIYANNIS‡

\*Department of Pharmacology and Toxicology and †Division of Biomedical Engineering,  
Virginia Commonwealth University, Box 613 MCV Station, Richmond, VA 23298-0613  
‡Department of Medicinal Chemistry, School of Pharmacy, and Institute of Materials Science,  
University of Connecticut, Storrs, CT 06269-2092

Received 4 December 1992

MARTIN, B. R., D. R. COMPTON, S. F. SEMUS, S. LIN, G. MARCINIAK, J. GRZYBOWSKA, A. CHARALAMBOUS AND A. MAKRIYANNIS. *Pharmacological evaluation of iodo and nitro analogs of  $\Delta^8$ -THC and  $\Delta^9$ -THC*. PHARMACOL BIOCHEM BEHAV 46(2) 295-301, 1993. — One aspect of cannabinoid structure-activity relationships (SARs) that has not been thoroughly investigated is the aromatic (A) ring. Although halogenation of the side chain enhances potency, our recent observation that iodination of the A ring also enhanced activity was surprising. The purpose of this investigation was to establish the steric and electrostatic requirements at these sites of the cannabinoid molecule via molecular modeling, while determining pharmacological activity. Molecular modeling was performed using the Tripos molecular mechanics force field and the semiempirical quantum mechanical package AM1. The  $K_i$  values for novel cannabinoids were determined in a [<sup>3</sup>H]CP-55,940 binding assay and ED<sub>50</sub> values generated from four different evaluations in a mouse model. The present studies underscore the increase in potency produced by a dimethylheptyl (DMH) side chain. Trifluoro substitutions on the pentyl side chain, or bromination of the DMH side chain, had little effect on the pharmacological activity. Any substitution at the C4 position of the aryl ring resulted in a loss of activity, which appears to be due to steric hindrances. Nitro, but not iodo, substitution at the C2 position essentially produces an inactive analog, and the drastic alteration of the electrostatic potential appears to be responsible. The altered pharmacological profile of the 2-iodo analog seems to be related to an alteration in the highest occupied molecular orbital because there is no alteration in the electron density map compared to  $\Delta^8$ -tetrahydrocannabinol.

$\Delta^9$ -Tetrahydrocannabinol    Structure-activity relationship    Locomotor activity    Rectal temperature  
Antinociception    Immobility    Binding    Molecular modeling    Analogs

SINCE the pioneering synthetic work of Roger Adams (1), it has been evident that structural modifications of the cannabinoid molecule profoundly influence the potency of this class of compounds. Indeed, the structure-activity (SAR) studies conducted by many investigators provided the first evidence for a cannabinoid receptor. Within a few short years, the in vitro binding characteristics of a cannabinoid receptor have been described (3), the location of these receptors in the brain has been mapped (6), and the receptor itself has been cloned (7). Although the amino acid sequence of this receptor is known, we do not know which portion of the receptor forms the binding domain and do not have information regarding the 3-D conformation of the receptor. Further refinement of the cannabinoid pharmacophore is essential for a number of reasons. Visualization of the pharmacophore will provide an avenue for design of agents with greater selectivity. The possibility that cannabinoid actions involve more than one canna-

binoid receptor can be pursued if there are discrepancies between biological activity and affinity for a particular binding site.

Considerable attention has been directed toward the three structural features of the cannabinoid molecule depicted in Fig. 1 (11). It has long been known that structural alterations at C9 influence potency and that removal or blockade of the phenolic hydroxyl at C1 essentially eliminates activity. Modifications of the side chain also dramatically alters activity. These observations have served well in depicting cannabinoid-receptor interactions; however, confining the description of these interactions to the basic structural requirements at these three sites is far too simplistic. Structurally diverse cannabinoids such as WIN 55,212-2 enforce this point (Fig. 1). One portion of the tetrahydrocannabinol (THC) molecule that has not been investigated thoroughly is the aromatic ring, which is most likely due to the fact that substitutions at the C2 and

<sup>1</sup> To whom requests for reprints should be addressed.

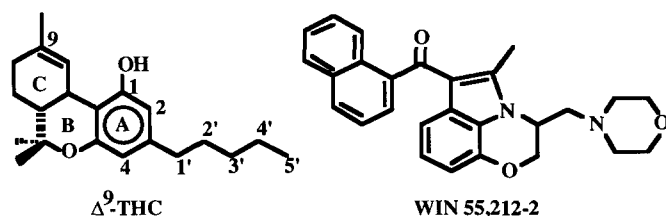


FIG. 1. Structure of  $\Delta^9$ -tetrahydrocannabinol and WIN 55,212-2.

C4 positions have rendered the cannabinoid inactive (8). Thus, our recent observation that iodination of  $\Delta^8$ -THC at the C2 position enhanced activity was indeed surprising (2). Additionally, both bromination and iodination in the side chain enhanced potency. The purpose of the present investigation was to extend these observations by establishing the steric and electrostatic requirements for these positions of the cannabinoid molecule via molecular modeling, while determining both *in vivo* and *in vitro* activity.

#### METHOD

##### Animals

Male ICR mice (22–30 g) obtained from Dominion Laboratories (Dublin, VA) were maintained on a 14 L : 10 D cycle and received food and water *ad lib*.

##### Drug Preparation and Administration

$\Delta^8$ -THC,  $\Delta^9$ -THC, and cannabidiol (CBD) were obtained from the National Institute on Drug Abuse and 4-bromo- $\Delta^8$ -THC was kindly supplied by Dr. Raj Razdan (Organix, Inc.). All other compounds were synthesized at the University of Connecticut (Storrs, CT) by methods similar to those previously reported for related cannabinoid analogs (2). Micellar suspensions of all compounds were prepared as described previously (9). The cannabinoids were dissolved by sonication in a 1 : 1 mixture of ethanol and emulphor (EL-620, a polyoxyethylated vegetable oil, GAF Corp., Linden, NJ). For IV injections, saline (0.9% NaCl) was added to this mixture to produce a 1 : 1 : 18 ratio of ethanol:emulphor:saline. This solution was diluted further with vehicle (1 : 1 : 18) to give the desired drug concentration.

##### Behavioral Evaluations

Mice were acclimated in the observation room (ambient temperature 20–24°C) overnight. Prior to vehicle or drug administration, rectal temperature was determined by a thermistor probe (inserted 25 mm) and a telethermometer (Yellow Springs Instrument Co., Yellow Springs, OH). The latency period (seconds) in the tail-flick procedure was measured as described by Dewey et al. (4). The heat lamp of the tail-flick apparatus was maintained at an intensity sufficient to produce control latencies of 2–4 s. Mice received tail-vein injections (0.1 ml/10 g) 5 min prior to being placed into individual photocell activity chambers. Spontaneous activity was measured for a 10-min period in a Digiscan Animal Activity Monitor (Omnitech Electronics, Inc., Columbus, OH) as the number of interruptions of 16 photocell beams per chamber and expressed as % control activity. Tail-flick latency was assessed again at 20 min after injection, and the change in the latency period (seconds) for each mouse was recorded. An automatic heat lamp cut-off time of 10 s was used to avoid tail injury.

Rectal temperature was measured again at 60 min after injection, and the difference between pre- and postinjection values ( $\Delta^\circ\text{C}$ ) was calculated for each animal.

Mice were evaluated for immobility 1.5 h after injection utilizing a slight modification of the procedure described by Pertwee (10). The test apparatus consisted of a 5.5-cm ring attached at a height of 16 cm to a ring stand. Each mouse was placed on a ring for 5 min. The total time the mouse remained motionless was recorded to the nearest second. This value was divided by 300 s and multiplied by 100 to obtain a % immobility rating. The only observable movements allowed during a period of "immobility" were gross body movements due to breathing. If a mouse escaped from the ring by jumping or falling (due to ataxia or sedation) more than five times, the evaluation of that animal was terminated and the immobility index was based upon the total time the mouse remained on the ring. Data from mice that did not remain on the ring at least 2.5 min prior to five escapes were disregarded.

##### Data Analysis

Depression of locomotor activity, hypothermia, antinociception, and ring immobility were expressed as % control activity,  $\Delta^\circ\text{C}$ , % maximum possible effect (%MPE) and % immobility, respectively. Antinociception was calculated as described by Dewey et al. (4). The %MPE data were converted to probit values for determination of the  $\text{ED}_{50}$  (or  $\text{MPE}_{50}$ ) by unweighted least-squares linear regression analysis of the log dose vs. probit plot. A theoretical maximum effect on locomotor activity, rectal temperature, and immobility was calculated from double-reciprocal analysis (1/effect vs. 1/dose) as described by Tallarida and Murray (12). The fractional response for each dose of drug was calculated (based upon the maximum effect being 1.0 for each individual behavioral measure), converted to probit values, and the  $\text{ED}_{50}$  determined by unweighted least-squares linear regression analysis of the log dose vs. probit plot.

##### In Vitro Binding Assays

The filtration procedure used for [ $^3\text{H}$ ]CP-55,940 binding is a modification of the centrifugation method described by Devane et al. (3). For a typical membrane preparation, five rats were decapitated and their cortices rapidly dissected free and homogenized in 30 ml 0.32 M sucrose that contained 2 mM EDTA and 5 mM  $\text{MgCl}_2$ . The homogenate was centrifuged at  $1,600\times g$  for 10 min and the supernatant removed. The pellet was washed twice by resuspending in 0.32 M sucrose/2 mM EDTA/5 mM  $\text{MgCl}_2$  and centrifuging again as described above. The original supernatant was combined with the wash supernatants and centrifuged at  $39,000\times g$  for 15 min. The resulting P2 pellet was suspended in 50 ml buffer (50 mM Tris HCl, pH 7.0, 2 mM EDTA, 5 mM  $\text{MgCl}_2$ ) and incubated at 37°C for 10 min before centrifugation at  $23,000\times g$  for 10 min. The P2 pellet was resuspended in 50 ml 50 mM Tris HCl/2 mM EDTA/5 mM  $\text{MgCl}_2$  and incubated at 30°C for 10 min before centrifugation at  $11,000\times g$  for 15 min. The final pellet was resuspended in 10 ml 50 mM Tris HCl (pH 7.4) that contained 1 mM EDTA and 3 mM  $\text{MgCl}_2$  and then stored at  $-40^\circ\text{C}$ . The binding assay was performed in silanized glass tubes that contained 100  $\mu\text{l}$  radiolabeled ligand, 100  $\mu\text{l}$  competing unlabeled drug, 150  $\mu\text{g}$  membrane protein (75  $\mu\text{l}$ ), and sufficient buffer [50 mM Tris HCl, pH 7.4, 1 mM EDTA, 3 mM  $\text{MgCl}_2$ , and 5 mg/ml bovine serum albumin (BSA)] to make a final volume of 1 ml. After a 1-h incubation at 30°C, the reaction was terminated by the addition of 2 ml ice-cold 50 mM Tris HCl (pH 7.4) buffer contain-

ing 1 mg BSA/ml and rapid filtration through polyethyleneimine-treated Whatman GF/C glass-fiber filters. The reaction tube was washed with a 2-ml aliquot of buffer that was then also filtered. The filters were washed with two 4-ml aliquots of ice-cold buffer. The filters were shaken for 60 min in 10 ml scintillation fluid and radioactivity quantitated by liquid scintillation spectrometry. Specific binding was typically 74% of total binding at 1 nM of tritiated ligand and was defined as the difference between the binding that occurred in the presence and absence of 1  $\mu$ M unlabeled ligand. The  $B_{max}$  and  $K_d$  values were obtained from Scatchard analysis as determined via the Ligand program of the KELL software package (Bio-soft, Milltown, NJ). Displacement  $K_i$  values were determined via the EBDA program of the KELL software package.

### Molecular Modeling

The molecular structures were constructed using the Sybyl 5.5 suite of programs as previously described (13). Geometry optimization was initially afforded by use of the Tripos molecular mechanics force field. Further geometry refinement, charge, and molecular orbital calculation was performed using the semiempirical quantum mechanical package AM1. Calculations were performed on the analogs of  $\Delta^8$ -THC, with reference to the parent unsubstituted compound. Electrostatic potential maps were generated for each analog with contouring at +1 and -1 kcal levels.

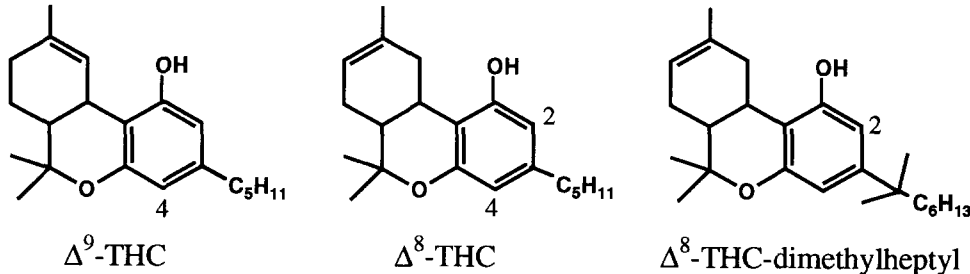
### RESULTS

The  $ED_{50}$  values in Table 1 show that  $\Delta^9$ -THC is equally effective in altering the four behavioral measures in mice and

that it competes with [ $^3$ H]CP 55,940 binding with a  $K_i$  of 41 nM. Determination of  $ED_{50}$  values for  $\Delta^9$ -THC was accomplished following establishment of dose-response curves (seven doses between 0.1 and 30 mg/kg), with subsequent regression analysis ( $R$ , correlation coefficient;  $n$ , number of doses per analysis) of spontaneous activity ( $R = 0.93$ ;  $n = 5$ ), tail-flick ( $R = 0.97$ ;  $n = 7$ ), temperature ( $R = 0.95$ ;  $n = 7$ ), and immobility ( $R = 0.97$ ;  $n = 7$ ) measures, as described in the Method section.  $\Delta^8$ -THC exhibits a similar profile (Table 1) and has approximately the same potency as  $\Delta^9$ -THC. Determination of  $ED_{50}$  values for  $\Delta^8$ -THC was accomplished following establishment of dose-response curves (six doses between 0.3 and 20 mg/kg), with subsequent regression analysis of spontaneous activity ( $R = 0.98$ ;  $n = 6$ ), tail-flick ( $R = 0.89$ ;  $n = 7$ ), temperature ( $R = 0.95$ ;  $n = 6$ ), and immobility ( $R = 0.98$ ;  $n = 6$ ) measures. Substitution of the pentyl side chain of  $\Delta^8$ -THC with a 1,1-dimethylheptyl side chain increases the potency approximately 30-fold in most behavioral assays with the exception of spontaneous activity, which was increased only 10-fold (Table 1).  $ED_{50}$  values for  $\Delta^8$ -THC-dimethylheptyl (DMH) was determined following establishment of dose-response curves (four doses between 0.03 and 1.0 mg/kg), with subsequent regression analysis of all measures ( $R > 0.94$ ;  $n = 4$ ). These results are consistent with previous observations that substitution of the pentyl side chain with a dimethylheptyl side chain increases potency (11).

Addition of an iodine at position C2 resulted in an alteration of the pharmacological profile.  $ED_{50}$  values for 2-iodo- $\Delta^8$ -THC were determined from dose-response curves (seven doses between 0.1 and 100 mg/kg), with subsequent regression

TABLE 1  
PHARMACOLOGICAL ACTIVITY OF CANNABINOIDS WITH SUBSTITUTIONS AT  
C2 AND C4 IN THE AROMATIC RING.



	Spontaneous Activity ( $\mu$ mol/kg)	Tail Flick ( $\mu$ mol/kg)	Temperature ( $\mu$ mol/kg)	Immobility ( $\mu$ mol/kg)	$K_i$ (nM)
<b>Standards</b>					
$\Delta^9$ -THC	3.2	4.5	4.5	4.8	41 $\pm$ 2
$\Delta^8$ -THC	2.9	4.8	4.5	4.8	44 $\pm$ 12
$\Delta^8$ -THC-DMH	0.27	0.14	0.15	0.17	0.77 $\pm$ 0.11
<b>Substitutions at C2 and C4</b>					
2-Iodo- $\Delta^8$ -THC*	8.0	0.68	20	4.3	89 $\pm$ 15
4-Bromo- $\Delta^8$ -THC	>250	>250	>250	>250	5,250 $\pm$ 2090
2,4-Diiodo- $\Delta^8$ -THC	>175	>175	>175	>175	10,600 $\pm$ 2,090
2-Nitro- $\Delta^8$ -THC	28.7	278	101	>300	>10,000
4-Nitro- $\Delta^8$ -THC	>275	>275	40.1	52.7	1,630 $\pm$ 360
2,4-Dinitro- $\Delta^8$ -THC	>75	>75	>75	>75	>10,000
2-Iodo- $\Delta^8$ -THC-DMH	4.4	5.0	10	1.7	61 $\pm$ 9

\*Previously reported by Charalambous et al. (2).



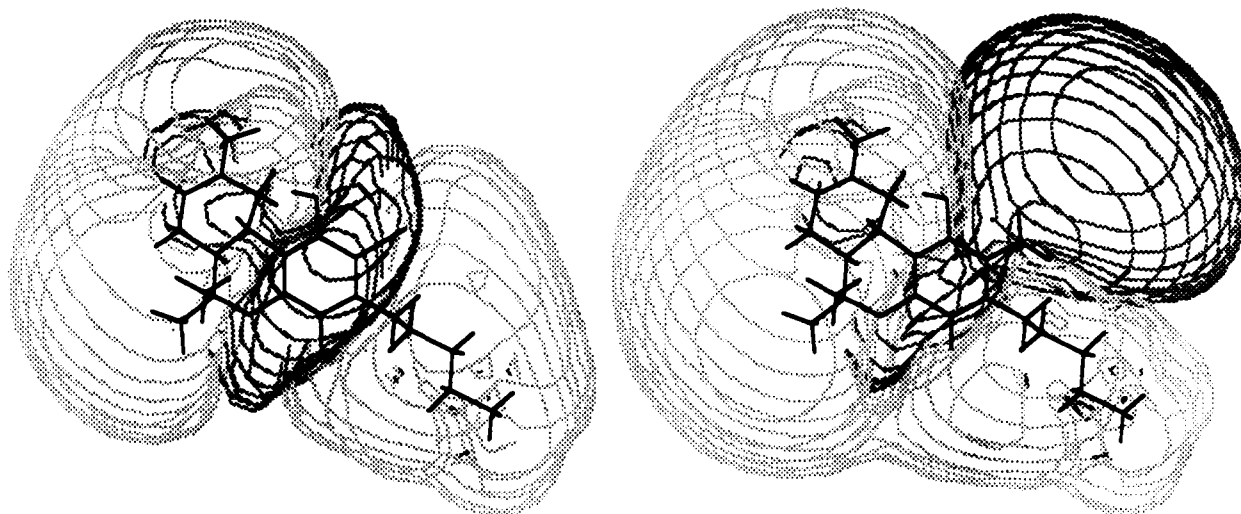


FIG. 2. Electrostatic potential maps of 2-iodo- (left) and 2-nitro- $\Delta^8$ -tetrahydrocannabinol (right). Dark contours indicate regions of high electron density and light contours highlight areas of electron deficiency.

quent regression analysis of all measures ( $R > 0.91$ ). It was anticipated that addition of a DMH side chain would dramatically increase the potency of 2-iodo- $\Delta^8$ -THC, as observed with  $\Delta^8$ -THC. On the contrary, the potency of 2-iodo- $\Delta^8$ -THC-DMH was only comparable to that of  $\Delta^8$ -THC and  $\Delta^9$ -THC.

Substitution of fluorines for hydrogens at the C5' position (Table 2) had relatively little effect on the pharmacological profiles of  $\Delta^9$ -THC,  $\Delta^8$ -THC, and CBD. The values for  $\Delta^9$ -THC and  $\Delta^8$ -THC in Table 2 are those given in Table 1 and reproduced for easier comparisons.  $ED_{50}$  values for CBD were determined from dose-response curves (four doses between 3.0 and 100 mg/kg), with subsequent regression analysis of spontaneous activity ( $R = 0.99$ ;  $n = 4$ ), tail-flick ( $R = 0.99$ ;  $n = 4$ ), temperature ( $R = 0.97$ ;  $n = 4$ ), and immo-

ility ( $R = 0.94$ ;  $n = 4$ ) measures. Differences between 5'-F<sub>3</sub>- $\Delta^9$ -THC and  $\Delta^9$ -THC across both in vivo and in vitro results were minimal. The only notable differences between 5'-F<sub>3</sub>- $\Delta^8$ -THC and  $\Delta^8$ -THC were the 4- and 10-times greater potency in spontaneous activity and tail-flick responses, respectively.  $ED_{50}$  values for both trifluoro analogs were determined from dose-response curves (six doses between 0.1 and 30 mg/kg), with subsequent regression analysis of all measures ( $R > 0.95$  or  $> 0.92$  for the  $\Delta^9$ - or  $\Delta^8$ -analog, respectively). The weak potency of CBD was not enhanced by trifluoro substitution at C5', although only doses up to 30 mg/kg could be evaluated. The exception to this generality is the fact that the  $ED_{50}$  in the tail-flick response for 5''-F<sub>3</sub>-CBD ( $R = 0.93$ ;  $n = 4$ ) was 18 times smaller than that for CBD.

As can be seen in Table 1, substitution of a DMH side

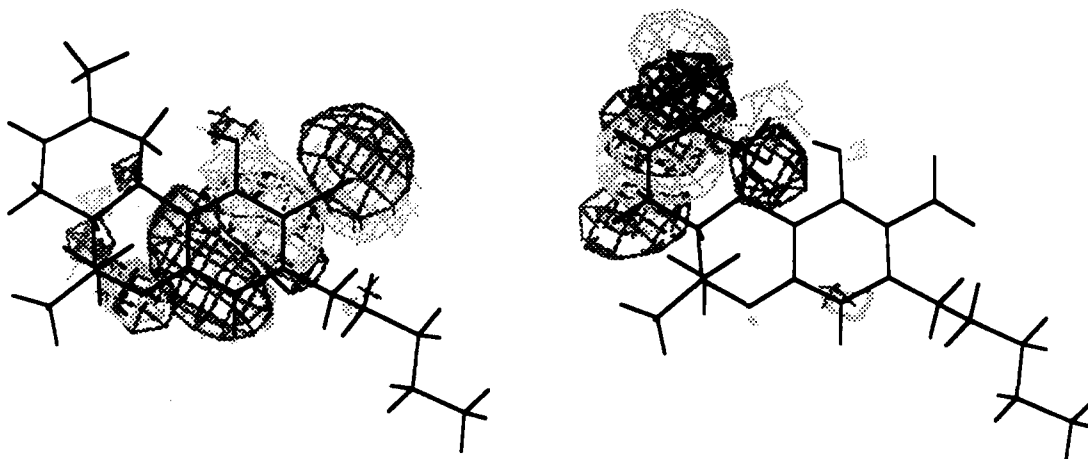


FIG. 3. Highest occupied molecular orbitals (HOMOs) of 2-iodo- (left) and 2-nitro- $\Delta^8$ -tetrahydrocannabinol (right) are indicated by the shaded areas.

chain for the pentyl side chain in  $\Delta^8$ -THC increases potency dramatically (10–30 times). The addition of a bromine to C7' of the DMH side chain had no influence on potency in any of the behavioral measures (Table 2). ED<sub>50</sub> values were generated from dose–response curves (six doses from 0.01 to 3 mg/kg) with regression analysis ( $R > 0.96$  for all measures). However, it was unexpected that substitution of a bromine on the C5' position of a dimethylpentyl side chain would result in a compound that was approximately two to three times more potent than either  $\Delta^8$ -THC-DMH or 7'-bromo- $\Delta^8$ -THC-DMH. ED<sub>50</sub> values for the dimethylpentyl analog were generated from dose–response curves (seven doses from 0.01 to 10 mg/kg) with subsequent regression analysis ( $R > 0.94$  for all measures).

Results from the molecular modeling studies are presented in Figs. 2 and 3. Examination of the electron density map for  $\Delta^8$ -THC revealed an electron-rich area surrounding the aromatic A ring and encompassing both the phenolic hydroxyl moiety and the B ring oxygen. Areas of electron deficiency are associated with the C ring and the C3 alkyl side chain. The iodine-substituted compounds (Fig. 2) show essentially the same features (electron-rich areas depicted by dark contours and electron-deficient areas indicated by light contours). The nitro-substituted analogs, however, present an altered electrostatic pattern, due in large part to the strong electron withdrawing power of this group. The C2- and C4-substituted analogs are *para* with respect to the oxygen atoms of the phenol and B ring and pull electrons from these moieties. Electron-rich areas in 2-nitro- $\Delta^8$ -THC are associated with the aromatic A ring and the nitro substituent, but electrons have been drawn away from the B ring oxygen, which is no longer part of this region. The electron deficient area is similar to the parent compound, although it now encompasses more of the B ring. 4-Nitro- $\Delta^8$ -THC presents a comparable picture, with the nitro group withdrawing electrons from the phenolic hydroxyl, thus reducing the electron population at this position. The 2,4-dinitro- $\Delta^8$ -THC analog is a combination of the two, with the electron-rich areas now almost entirely associated with just the nitro groups and the electron-deficient region spreading from the C ring across both the B and A rings to the alkyl side chain. Besides determination of the electron density contour maps, consideration of the highest occupied molecular orbital (HOMO) for this series of compounds was determined. The results are presented in Fig. 3, and the reasons for these determinations are given in the Discussion section, where their importance is discussed.

#### DISCUSSION

The present studies further underscore the importance of the side chain in the actions of the cannabinoids. Substitution of fluorines for the hydrogens on C5' (or C5'') of the straight pentyl side chain had relatively little effect on the pharmacological activity of the THCs or CBD, likely due to the fact that both fluorine and hydrogen atoms occupy comparable volumes despite differences in their electrostatic properties. Similarly, although branching or extending the side chain markedly increases potency in general the addition of a bromine to the terminus of the DMH side chain also had no influence on potency. This observation is also consistent with the findings of Mechoulam and Ederly (8), who demonstrated that potency is retained even when the side chain is extended up to eight carbon atoms. It is an interesting contrast that although  $\Delta^8$ -THC-dimethylpentyl was not available for comparison it appears bromination of this molecule potentiates

pharmacological activity because 5'-bromo- $\Delta^8$ -THC-DMH appears to be even more potent than  $\Delta^8$ -THC-DMH itself.

There is a basic underlying assumption that for a series of analogs to interact at the same receptor site they will present a common steric and electrostatic pattern. Early studies by Ederly and Mechoulam (5) showed that substitutions of strongly electronegative groups at positions C2 and C4 rendered the cannabinoid inactive. On the other hand, substitution in position C2 of the A ring by both methyl and ethyl groups was tolerated (5). Substitution at position C4 by any group was not tolerated and may well indicate a place of steric interaction with the receptor site. Despite these observations, the importance of positions C2 and C4 have not been evaluated critically for their role in ligand–receptor interaction. Alterations in the electron density map of  $\Delta^8$ -THC by addition of a nitro at C2, but not by iodination, suggests that electron densities of the phenol and the oxygen in the B ring are essential for activity. This observation was reinforced in 4-nitro- and 2,4-dinitro- $\Delta^8$ -THC.

Where there is a common electrostatic pattern but different pharmacological activity (as is the case between the iodo analogs and the parent compound), examination of the molecular orbitals can provide insight into the potential mode of interaction of such analogs in binding. The HOMO calculation represents the orbital of a molecule (drug) occupied by an electron that is closest in energy to the unoccupied orbitals of another molecule (such as a receptor), and could represent the critical characteristic in the binding interaction. Conversely, it could be the lowest unoccupied molecular orbital of a molecule (drug) that represents the empty orbital to which a donor molecule (such as a receptor) might interact. The potential interaction of these frontier orbitals need to be considered because the energetic effects of such two-electron interactions (i.e., that of a filled orbital with an empty one) are far larger than those of interactions involving four electrons. In  $\Delta^8$ -THC, the HOMO encompasses the aromatic A ring together with the phenolic hydroxyl group and the B ring oxygen. The iodo-substituted compounds demonstrate a similar profile that additionally includes the iodine atom in the HOMO (Fig. 3). This pattern would suggest that the enhanced activity of 2-iodo- $\Delta^8$ -THC may be a result of direct interaction of the iodine atom with a subsite on the receptor. Both the 2-nitro and 2,4-dinitro analogs, however, show a dramatically different HOMO that is concentrated largely around the C ring. This shift from the A and B rings in these molecules may explain their biological inactivity. The 4-nitro analog is unusual in that although its electrostatic pattern is similar to the other nitro compounds its HOMO is similar to  $\Delta^8$ -THC but with the additional incorporation of the nitro group. This would seem to suggest that there is some steric interference with binding, which could further explain the relative inactivity of 2,4-disubstituted compounds.

It will now be important to design analogs that will (presumably) exert a predictable influence on the proposed electrostatic and HOMO maps to test the validity of these assumptions. The observation that substitutions at position C2 are possible that can favorably alter electrostatic charges without producing unfavorable steric influences will play a key role in this endeavor.

#### ACKNOWLEDGEMENTS

This research was supported by NIDA Grants DA 03672 and DA 05488 and The Commonwealth of Virginia Center on Drug Abuse Research. The authors are indebted to Renee Jefferson, Ramona Winckler, and Troy Bridgen for excellent technical assistance.

## REFERENCES

1. Adams, R. *Marihuana*. Harvey Lect. 37:168-197; 1942.
2. Charalambous, A.; Lin, S.; Marciniak, G.; Banijamali, A.; Friend, F. L.; Compton, D. R.; Martin, B. R.; Makriyannis, A. Pharmacological evaluation of halogenated delta-8-THC analogs. *Pharmacol. Biochem. Behav.* 40:509-512; 1991.
3. Devane, W. A.; Dysarz, I., F. A.; Johnson, M. R.; Melvin, L. S.; Howlett, A. C. Determination and characterization of a cannabinoid receptor in rat brain. *Mol. Pharmacol.* 34:605-613; 1988.
4. Dewey, W. L.; Harris, L. S.; Howes, J. F.; Nuite, J. A. The effect of various neurohumoral modulators on the activity of morphine and the narcotic antagonists in the tail-flick and phenylquinone tests. *J. Pharmacol. Exp. Ther.* 175:435-42; 1970.
5. Edery, H.; Grunfeld, Y.; Porath, G.; Ben-Zvi, Z.; Shani, A.; Mechoulam, R. Structure-activity relationships in the tetrahydrocannabinol series. *Arzneim-Forsch.* 22:1995-2003; 1972.
6. Herkenham, M.; Lynn, A. B.; Little, M. D.; Johnson, M. R.; Melvin, L. S.; DeCosta, B. R.; Rice, K. C. Cannabinoid receptor localization in the brain. *Proc. Natl. Acad. Sci. USA* 87:1932-1936; 1990.
7. Matsuda, L. A.; Lolait, S. J.; Brownstein, M. J.; Young, A. C.; Bonner, T. I. Structure of a cannabinoid receptor and functional expression of the cloned cDNA. *Nature* 346:561-564; 1990.
8. Mechoulam, R.; Edery, H. Structure-activity relationships in the cannabinoid series. In: Mechoulam, R., ed. *Marijuana chemistry, pharmacology, metabolism, and clinical effects*. New York: Academic Press; 1973:101-136.
9. Olson, J. L.; Makhani, M.; Davis, K. H.; Wall, M. E. Preparation of  $\Delta^9$ -tetrahydrocannabinol for intravenous injection. *J. Pharm. Pharmacol.* 25:344; 1973.
10. Pertwee, R. G. The ring test: A quantitative method for assessing the "cataleptic" effect of cannabis in mice. *Br. J. Pharmacol.* 46:753-63; 1972.
11. Razdan, R. K. Structure-activity relationships in cannabinoids. *Pharmacol. Rev.* 38:75-149; 1986.
12. Tallarida, R. J.; Murray, R. B. Graded dose-response. In: Tallarida, R. J.; Murry, R. B., ed. *Manual of pharmacologic calculations*. New York: Springer-Verlag; 1987:26-31.
13. Thomas, B. F.; Compton, D. R.; Martin, B. R.; Semus, S. F. Modeling the cannabinoid receptor: A three-dimensional quantitative structure-activity analysis. *Mol. Pharmacol.* 40:656-665; 1991.